

On the toroidal-velocity anti-dynamo theorem under the presence of nonuniform electric conductivity

G. Rüdiger^{1,2*} and M. Schultz¹

¹Leibniz-Institut für Astrophysik Potsdam, An der Sternwarte 16, 14482 Potsdam, Germany

²University of Potsdam, Institute of Physics and Astronomy, Karl-Liebknecht-Str. 24-25, 14476 Potsdam, Germany

Received 01 July 2021, accepted later

Published online later

Key words MHD, Taylor-Couette flow, dynamo anti-theorem

Laminar electrically conducting Couette flows with quasi-Keplerian rotation law and nonuniform conductivity are probed for dynamo instability. In spherical geometry the equations for the poloidal and the toroidal field components completely decouple resulting in free decay independent of the spatial distribution of the electric conductivity. For cylindrical flows the decoupling vanishes but also here we do not find dynamo excitations for the two cases that the electric conductivity only depends on the radius or – much more complex – that it only depends on the azimuth. The transformation of the plane-flow dynamo model of Busse & Wicht (1992) to cylindrical or spherical geometry, therefore, fails. It is also shown that even the inclusion of axial flows of both signs does *not* support the dynamo mechanism. The Elsasser toroidal-velocity antidynamo theorem, after which dynamos without any radial velocity component cannot work, is thus not softened by nonuniform conductivity distributions.

Copyright line will be provided by the publisher

1 Introduction

It has been demonstrated by Busse & Wicht (1992) that a large-scale magnetic field can be excited by a slab dynamo formed by a plane laminar shear flow and an electric conductivity which is sinusoidally modulated in stream-wise direction. The flow becomes supercritical for rather large magnetic Reynolds number of order $10^{4\dots 5}$ which can be optimized when the perturbation scale of the magnetic field approaches the scale of the conductivity variations where the latter may exceed the thickness of the slab. If, on the other hand, the electric conductivity varied crosswise rather than streamwise no dynamo effect has been found by the authors.

Another question is whether this positive result can be transformed to cylindrical and/or spherical geometry. If yes then a dynamo should also work for differential rotation of a fluid of nonuniform electric conductivity. Then dynamo action should be possible for non-rigidly rotating cylinders or spheres with nonuniform conductivity distribution in azimuthal direction. It is known, however, that spherical dynamos with only toroidal internal flows do not exist for uniform conductivity distribution (Elsasser 1946; Ivers & James 1988b; Kaiser & Busse 2017).

In this case differential rotation is not enough to form a dynamo mechanism but, as suggested by Gailitis (1970) pure meridional flow should be enough for sufficiently large magnetic Reynolds number of the flow (Latter & Ivers 2010; Moss 2006). Dudley & James (1989) demonstrated how the addition of differential rotation to the meridional

flow can strongly reduce the critical magnetic Reynolds number for suitable amplitude ratios of the flow components.

One can easily show that for spheres the differential-rotation anti-dynamo theorem also holds for nonuniform conductivity distribution. The induction equation for a laminar magnetized fluid with a finite magnetic resistivity $\eta = 1/\mu\sigma$ (with σ as its electric conductivity) reads

$$\frac{\partial \mathbf{B}}{\partial t} = \text{curl}(\mathbf{u} \times \mathbf{B} - \eta \text{curl} \mathbf{B}), \quad (1)$$

with $\text{div} \mathbf{u} = \text{div} \mathbf{B} = 0$ for an incompressible fluid and \mathbf{u} as its velocity. \mathbf{B} is the magnetic field, here the magnetic resistivity is not necessarily uniform. The question is whether for given mean flow this equation, which is homogeneous in the magnetic field, has eigenvalues with marginal growth rates.

Following the method demonstrated in the textbook of Krause & Rädler (1980) the induction equation in spheres is split into a poloidal and a toroidal component by use of the poloidal field component $\text{curl} \mathbf{A}_{\text{tor}}$ and the toroidal field component \mathbf{B}_{tor} with

$$\mathbf{A}_{\text{tor}} = -\mathbf{r} \times \nabla S \quad \mathbf{B}_{\text{tor}} = -\mathbf{r} \times \nabla T \quad (2)$$

with \mathbf{r} as the radial vector $\mathbf{r} = (r, 0, 0)$ in spherical geometry. Two equations for S and T are resulting. Here only the relation

$$\frac{\partial S}{\partial t} + \Omega \frac{\partial S}{\partial \phi} - \eta \Delta S = U_{\text{ind}}, \quad (3)$$

for the poloidal field component S may be considered, where Ω is the (nonuniform) rotation rate of the sphere. The RHS of this equation describes the induction by the mean circulation \mathbf{u}^{m} , i.e.

$$\mathcal{L}U_{\text{ind}} = -\mathbf{r} \cdot \text{curl} \mathbf{u}^{\text{m}} \times \mathbf{B}. \quad (4)$$

* E-mail: GRuediger@aip.de

The operators Δ and \mathcal{L} ,

$$\begin{aligned}\Delta &= \frac{1}{r^2} \left(\frac{\partial}{\partial r} \left(r^2 \frac{\partial}{\partial r} \right) + \mathcal{L} \right), \\ \mathcal{L} &= \frac{1}{\sin \theta} \frac{\partial}{\partial \theta} \left(\sin \theta \frac{\partial}{\partial \theta} \right) + \frac{1}{\sin^2 \theta} \frac{\partial^2}{\partial \phi^2}\end{aligned}\quad (5)$$

are well-known. From Eq. (4) one finds the explicit formulation

$$\begin{aligned}\mathcal{L}\mathcal{U}_{\text{ind}} &= -\nabla(r\mathbf{u}_r) \cdot \mathbf{r} \times \nabla T - \mathbf{u}^m \nabla \mathcal{L}S + \\ &+ u_r(r\Delta S + \nabla \frac{\partial}{\partial r}(rS)).\end{aligned}\quad (6)$$

The striking result is that only the first term of the RHS of this relation is able to couple the toroidal field by Eq. (3) but this term vanishes for $u_r = 0$. Without this source term the relation (3) is homogeneous in S and only describes the decay of this field component independent of the actual form of the function η (Ivers & James 1988a). A self-maintaining nonturbulent dynamo in spherical geometry is thus only possible for flows with finite radial component, i.e. including meridional flows. This is a known anti-dynamo theorem which obviously even holds for nonuniform distributions with $\eta > 0$. The transformation of the plane dynamo model of Busse & Wicht (1992) working with streamwise η -modulation between two narrow plates to spherical geometry is thus not possible. Kaiser & Busse (2017) have shown that this toroidal-velocity anti-dynamo theorem also survives up to a certain nonradial resistivity variation which decreases for increasing magnetic Reynolds numbers. The existence of this limit characterizes the robustness of the toroidal anti-dynamo theorem, dynamo excitation, therefore, is not excluded by this analysis for large enough resistivity variations.

This might support the idea of Rogers & McElwaine (2017) that a dynamo can basically work in the thin stably stratified atmosphere of a hot Jupiter on the basis of strong conductivity variations due to the heating of the near host star. After the findings of the present paper, however, even this dynamo can only operate under the presence of differential rotation *and* meridional circulation. Detailed calculations of the wind system in ultra-hot Jupiters have been published by Tan & Komacek (2019).

For nonuniform magnetic resistivity the induction equation reads

$$\frac{\partial \mathbf{B}}{\partial t} = \text{curl}(\mathbf{u} \times \mathbf{B}) + \eta \Delta \mathbf{B} - \nabla \eta \times \text{curl} \mathbf{B} \quad (7)$$

(Giesecke et al. 2010; Rogers & McElwaine 2017). It has been argued that the last term of this equation can formally be considered as a new alpha-effect term necessary for dynamo operation. It is, however, perpendicular to the electric current $\text{curl} \mathbf{B}$ while the corresponding term by an alpha effect is parallel to $\text{curl} \mathbf{B}$. One can show that one of the main consequences of this last term is the advection of magnetic field in direction of $\nabla \eta$. It is

$$\nabla \eta \times \text{curl} \mathbf{B} = \text{curl}(\nabla \eta \times \mathbf{B}) + \nabla(\nabla \eta \cdot \mathbf{B}) + \dots, \quad (8)$$

where the dots represent a tensor formed with second derivatives of η , i.e. $(\Delta \eta \delta_{ij} - 2\eta_{,ij})B_j$. The first term on the

RHS of this equation describes an advection of the field antiparallel to $\nabla \eta$ (see Eq. (1)), which is, if too strong, known to suppress dynamo action, see Krause & Rädler (1980) and Brandenburg et al. (1992). Also the remaining terms cannot play the role of an alpha effect. Always the existence of an alpha effect requires the existence of a pseudo-scalar or a pseudo-tensor.

It makes sense to inspect the radial component of (7) in spherical coordinates, i.e.

$$\begin{aligned}\frac{\partial B_r}{\partial t} + \Omega \frac{\partial B_r}{\partial \phi} &= \eta \left(\frac{1}{r} \frac{\partial^2}{\partial r^2} r B_r + \frac{1}{r^2} \frac{\partial^2 B_r}{\partial \theta^2} + \right. \\ &+ \frac{1}{r^2 \sin^2 \theta} \frac{\partial^2 B_r}{\partial \phi^2} + \frac{\cot \theta}{r^2} \frac{\partial B_r}{\partial \theta} + \frac{2}{r} \frac{\partial B_r}{\partial r} + \frac{2B_r}{r^2} \left. \right) - \\ &- \frac{1}{r^2} \frac{\partial \eta}{\partial \theta} \left(\frac{\partial}{\partial r} r B_\theta - \frac{\partial B_r}{\partial \theta} \right) + \\ &+ \frac{1}{r^2 \sin \theta} \frac{\partial \eta}{\partial \phi} \left(\frac{1}{\sin \theta} \frac{\partial B_r}{\partial \phi} - \frac{\partial}{\partial r} r B_\phi \right) + \dots\end{aligned}\quad (9)$$

All terms due to a meridional circulation have been cancelled. We note in particular for the last two lines of this expression the appearance of the ∇ -terms of (8). For strong shear the combination of $\partial \eta / \partial \phi$ with B_ϕ should make the strongest effect. A radial gradient of the resistivity does not appear explicitly.

2 Cylinder geometry

The negative conclusion for spherical geometry cannot automatically be transformed to cylinder geometry. A special situation exists for cylinder geometry as the operator $\text{curl} \text{curl}$ combines various magnetic field components, i.e.

$$\begin{aligned}\frac{\partial B_R}{\partial t} + \Omega \frac{\partial B_R}{\partial \phi} &= \eta \left(\frac{\partial}{\partial R} \left(\frac{1}{R} \frac{\partial}{\partial R} (R B_R) \right) + \frac{\partial^2 B_R}{\partial z^2} + \right. \\ &+ \left. \frac{1}{R^2} \frac{\partial^2 B_R}{\partial \phi^2} - \frac{2}{R^2} \frac{\partial B_\phi}{\partial \phi} \right) + \dots,\end{aligned}\quad (10)$$

written in cylinder coordinates (R, ϕ, z) . Obviously, in contrast to (9) for nonaxisymmetric fields a coupling exists between the azimuthal and the radial field components which might be able to enable a dynamo-selfexcitation in a similar sense as the $\Omega \times \mathbf{J}$ effect in turbulent dynamo theory does. The latter is part of the eddy-diffusivity tensor containing the linear-in- Ω influence on the magnetic dissipation. It is thus necessary to find out whether for cylindrical models the combination of differential rotation and nonuniform electric conductivity can be dynamo-active. Distances and wave numbers may be normalized with the outer cylinder radius R_0 and the inner cylinder measures $r_{\text{in}} R_0$. The rotation and other frequencies are normalized with the rotation rate Ω_{in} of the inner cylinder, the rotation rate of the outer cylinder is $\mu \Omega_{\text{in}}$. The rotation law may be written as

$$\Omega(R) = a_\Omega + \frac{b_\Omega}{R^2} \quad (11)$$

with

$$a_\Omega = \frac{\mu - r_{\text{in}}^2}{1 - r_{\text{in}}^2}, \quad b_\Omega = \frac{1 - \mu}{1 - r_{\text{in}}^2} r_{\text{in}}^2. \quad (12)$$

Here $\mu = \Omega_{\text{out}}/\Omega_{\text{in}}$ is the ratio of the rotation rates of the outer and the inner cylinder. For $\mu = r_{\text{in}}^{1.5}$ the cylinders rotate after the Kepler law, i.e. $\mu = 0.35$ for $r_{\text{in}} = 0.5$. The magnetic Reynolds number of the rotation is defined as

$$\text{Rm} = \frac{\Omega_{\text{in}} R_0^2}{\eta_0}, \quad (13)$$

where the η_0 is a characteristic value of the resistivity defined by the definition of the η -profile. The magnetic-field vector in cylinder coordinates is $\mathbf{B} = (A, B, B_z)$. The equations are solved by means of the Fourier series $A = \sum_m A_m(R) \exp i(kz + m\phi + \omega t)$ and $B = \sum_m B_m(R) \exp i(kz + m\phi + \omega t)$ while the axial field B_z is always substituted by means of the divergence condition. The solutions are assumed as periodic along the rotation axis, k is the wave number (a parameter) in this direction. ω is the eigenvalue of the system with its real part as the azimuthal drift rate and its negative imaginary part as the growth rate. Negative growth rate indicates decay of the magnetic pattern while vanishing growth rate marks neutral instability. In case of selfexcitation the wave number k can be used to find the optimal excitation condition.

The eigenfunctions and the eigenvalues fulfill the symmetry conditions

$$A_{-m} = A_m^*, \quad B_{-m} = B_m^* \quad \text{if} \quad \omega_{-m} = -\omega_m^*. \quad (14)$$

To normalize the growth rate with the diffusion time we have simply to write

$$\omega_{\text{gr}} = -\text{Rm} \omega^{\text{I}}. \quad (15)$$

If ω_{gr} does not depend on Rm and is of order unity then growth (or decay) of the modes are only directed by the diffusion scale. Negative values of (15) indicate decaying magnetic fields. All plots in this paper are using the growth rates described in these units. The same is true for the drift rates $d\phi/dt = -\omega_{\text{dr}}$ with

$$\omega_{\text{dr}} = \text{Rm} \omega^{\text{R}}. \quad (16)$$

Hence, $\omega_{\text{dr}} < 0$ implies azimuthal drift in positive direction.

For comparison both the decay and drift rates of infinite cylinders with uniform resistivity have been calculated with the results presented by Fig. 1. The upper panel concerns the decay of the modes with $m = 0$ (green lines) and $m = 1$ (red lines) for two different wave numbers $k = 1$ (solid lines) and $k = 2$ (dashed lines). Axisymmetric magnetic fields decay with the diffusion time scale, hence the influence of the differential rotation can be neglected. The non-axisymmetric mode with $m = 1$ decays even faster. Without rotation the resulting growth rates for $k = 1$ are $\omega_{\text{gr}} = -1$ for axisymmetric fields and $\omega_{\text{gr}} = -2.83$ for nonaxisymmetric fields with $m = 1$. For $k = 2$ the corresponding numbers are $\omega_{\text{gr}} = -4$ and $\omega_{\text{gr}} = -5.83$. In contrast to the decay law for $m = 0$, for $m = 1$ the influence of the magnetic Reynolds number is strong so that the physical decay rate scales with the rotation rate, $\omega_{\text{gr}} \propto -\Omega$. The decay time of nonaxisymmetric fields is strongly reduced by rotational shear independent of its sign. As the up-winding of the field lines by the differential rotation leads to shorter scales,

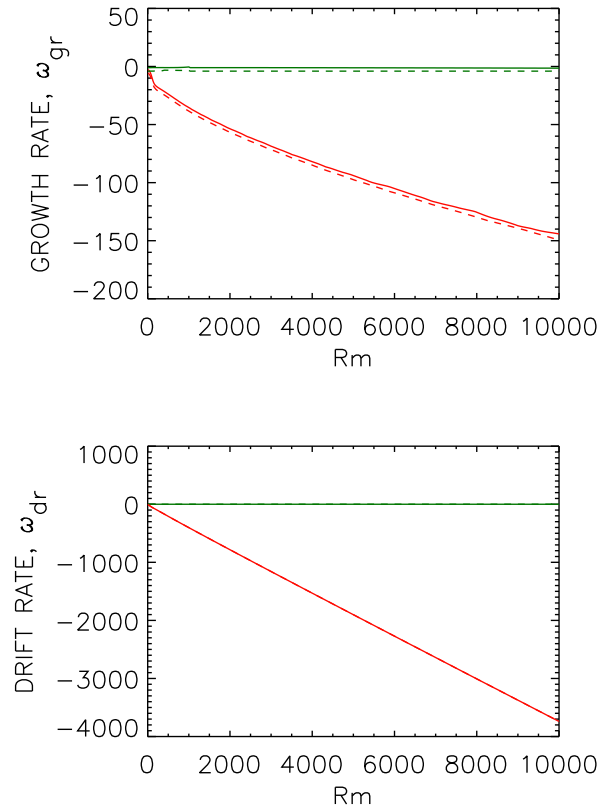


Fig. 1 For reference: the decay rates (top) and drift rates (bottom) in units of the diffusion time for uniform η and for $m = 0$ (green) and for $m = 1$ (red). Two different wave numbers $k = 1$ (solid), $k = 2$ (dashed). $r_{\text{in}} = 0.5$, $\mu = 0.35$ (Kepler rotation). Perfect-conducting boundary conditions.

for fast rotation the decay time becomes shorter (Krause & Rädler 1980). For high magnetic Reynolds numbers nonaxisymmetric fields decay $\sqrt{\text{Rm}}$ times faster than axisymmetric fields.

The azimuthal drift of an axisymmetric field, of course, vanishes while for nonaxisymmetric fields it basically drifts by the action of the differential rotation (bottom panel of Fig 1). The drift frequency for large Rm corresponds to the rotation rate of the outer cylinder, i.e. $\mu\Omega_{\text{in}}$. As formulated by Elsasser (1946) assuming uniform conductivity “for toroidal flow the induction effect consists in oscillatory changes of the field amplitudes superposed upon the slow, general decay of the field”.

In the following we shall demonstrate that these results are only slightly modified if the molecular resistivity η is no longer uniform. Here we distinguish between models with radial gradients of the molecular resistivity and models with azimuthal gradients. Axial gradients of η have not been considered in this paper as also Busse & Wicht did not find dynamo excitation for such models.

2.1 Radius-dependent conductivity

We start to consider a cylindric fluid with a radius-dependent magnetic resistivity. Write $\eta = \eta_0 \eta(R)$ with $\eta(R) = R^{-\mu_\eta}$ (hence $\eta(1) = 1$), where the profile parameter μ_η can have both signs. For positive values the electric conductivity grows outward (η grows inward). The model is rather simple as the radius-dependent magnetic resistivity does not lead to complicated mode couplings as in the model by Busse & Wicht (1992) or our below model with azimuth-dependent η . The equation system for four differential equations of first order is used formulated by Shal'bkov et al. (2002), i.e.

$$\frac{dA_m}{dR} - \left(k^2 + \frac{m^2}{R^2}\right)A_m - \frac{iRm}{\eta(R)}(\omega + m\Omega(R))A_m - \frac{2im}{R^2}B_m = 0, \quad (17)$$

$$\begin{aligned} \frac{dB_m}{dR} - \frac{\mu_\eta B_m}{R} - \left(k^2 + \frac{m^2}{R^2}\right)B_m - \frac{iRm}{\eta(R)}(\omega + m\Omega(R))B_m + \\ + (2 + \mu_\eta)\frac{imA_m}{R^2} - 2\frac{Rm b_\Omega}{\eta(R)R^2}A_m = 0 \end{aligned} \quad (18)$$

with

$$A_m = \frac{dA_m}{dR} + \frac{A_m}{R}, \quad B_m = \frac{dB_m}{dR} + \frac{B_m}{R}. \quad (19)$$

The boundary conditions for these equations are $A_m = B_m = 0$ for perfect-conducting walls at $R = r_{\text{in}}, 1$ or

$$\left(k^2 + \frac{m^2}{R^2}\right)B_m - \frac{imA_m}{R} = 0 \quad (20)$$

for vacuum conditions. In this case it is also

$$kA_m - \left(A_m + \frac{imB_m}{R}\right) \left(\frac{m}{kR} + \frac{I_{m+1}(kR)}{I_m(kR)}\right) = 0 \quad (21)$$

at $R = r_{\text{in}}$ and

$$kA_m - \left(A_m + \frac{imB_m}{R}\right) \left(\frac{m}{kR} - \frac{K_{m+1}(kR)}{K_m(kR)}\right) = 0 \quad (22)$$

at $R = 1$ (Rüdiger et al. 2018). We note that $I_{-m} = I_m$ and $K_{-m} = K_m$. Sometime also pseudo-vacuum conditions (vertical fields) $B_m = A_m = 0$ have been used at $R = r_{\text{in}}, 1$.

The decay rates for two models with Kepler rotation and with radial η -gradients of opposite signs are given in Fig. 2. The free axial wave numbers have been varied between $k = 0.1$ and $k = 1$ but the curves are almost identical. Magnetic modes with different wave numbers decay with the same rate – except for $Rm = 0$ where the modes with larger wave number (here $k = 1$) decay faster. The magnetic Reynolds number of the rotation is assumed as growing to very large numbers of $Rm \lesssim 10^4$. As expected for nonaxisymmetric fields under the influence of differential rotation the decay rate grows with growing magnetic Reynolds numbers, the decay frequency is thus proportional to the rotation rate hence $\tau_{\text{dec}} \propto \tau_{\text{in}}$ with τ_{in} as the rotation period of the

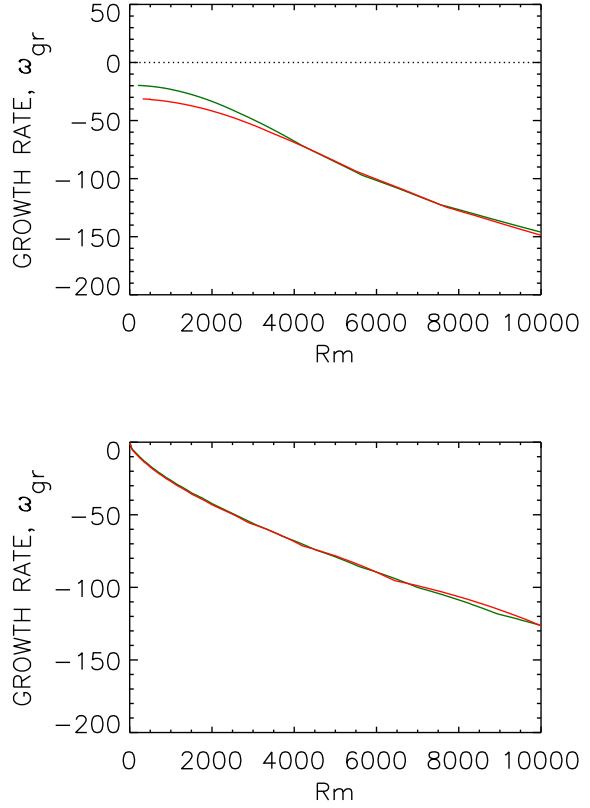


Fig. 2 The decay rates of the nonaxisymmetric mode ($m = 1$) in units of the diffusion time for two models of $\eta = \eta(R)$. Top: $\mu_\eta = 10$ (conductivity grows outward), insulating walls; Bottom: $\mu_\eta = -3$ (conductivity grows inward), perfect-conducting walls. Wave numbers $k = 0.1$ (green), $k = 1$ (red). $r_{\text{in}} = 0.5$, $\mu = 0.35$ (Kepler rotation).

inner cylinder. Short time scales are produced by the winding up of the field lines by the nonuniform rotation which decay faster the larger the value of Rm is. The decay rates for η increasing outwards or decreasing outwards do not differ basically. The influence of the sign of the η -gradient on the decay times is obviously weak. As it should, the decay is (slightly) faster for negative gradients, i.e. for $\mu_\eta > 0$. The drift rates (not shown) in both cases are almost identical to the values shown in the lower panel of Fig. 1. Independently of the basically different radial η -profiles the nonaxisymmetric field pattern always drifts with the rate Ω_{out} for large Rm .

The result is that a radial non-uniformity of conductivity even for large magnetic Reynolds numbers does not lead to any dynamo action (Ivers & James 1988a). Fig. 2 also shows that also a nonaxisymmetric field cannot be maintained only by differential rotation. The toroidal-velocity anti-dynamo theorem obviously also holds with cylindric geometry and arbitrary radial η -gradients. The curves do not show any indication that the trends are changed for higher magnetic Reynolds numbers. In agreement with Kaiser &

Table 1 Coefficients κ_n and $\bar{\kappa}_n$ for $\kappa = 0.5$ and $\kappa = 0.9$.

| mode n | $\kappa_n(0.5)$ | $\bar{\kappa}_n(0.5)$ | $\kappa_n(0.9)$ | $\bar{\kappa}_n(0.9)$ |
|----------|-----------------|-----------------------|-----------------|-----------------------|
| -3 | 0.019 | 0.022 | 0.25 | 0.56 |
| -2 | 0.072 | 0.083 | 0.39 | 0.96 |
| -1 | 0.27 | 0.31 | 0.63 | 1.44 |
| 0 | 0 | 1.15 | 0 | 2.29 |
| 1 | -0.27 | 0.31 | -0.63 | 1.44 |
| 2 | -0.072 | 0.083 | -0.39 | 0.96 |
| 3 | -0.019 | 0.022 | -0.25 | 0.56 |

Busse (2017) we do not find evidence for dynamo action of differential rotation in combination with radial η -gradients of both signs.

2.2 Azimuth-dependent conductivity

Models with nonradial variation of the η -profile are more complex. The reason is that in the nonradial coordinates z and ϕ the solutions are developed into Fourier modes and for resistivities varying in these directions the modes couple producing always an infinite series. Here we shall only provide solutions of the dynamo equation (1) for η as a function of the azimuth ϕ .

The azimuthal variation of the magnetic resistivity may be written as

$$\eta = \eta_0(1 - \kappa \cos \phi), \quad (23)$$

where the coefficient κ may vary between 0 and 1. The value η_0 is the average over the azimuth. The ratio of the maximum value of η and its minimum is simply $(1 + \kappa)/(1 - \kappa)$ so that it approaches large values for $\kappa \rightarrow 1$.

Ansatz (23) describes the consequences of a heating of the cylinder at a phase zero and a cooling at the opposite phase π . One could also work with higher azimuthal frequencies by replacing $\cos \phi$ in (23) by $\cos N\phi$. In all cases with $\kappa \neq 0$ the magnetic modes with the azimuthal wave number m are coupling so that an infinite set of equations results. The coupling coefficients are

$$\begin{aligned} \kappa_n &= \frac{i\kappa}{2\pi} \int_0^{2\pi} \frac{\sin \phi e^{in\phi}}{1 - \kappa \cos \phi} d\phi, \\ \bar{\kappa}_n &= \frac{1}{2\pi} \int_0^{2\pi} \frac{e^{in\phi}}{1 - \kappa \cos \phi} d\phi. \end{aligned} \quad (24)$$

The κ_n and $\bar{\kappa}_n$ are real numbers with $\kappa_{-n} = -\kappa_n$ and $\bar{\kappa}_{-n} = \bar{\kappa}_n$. For $\kappa = 0$ it is $\bar{\kappa}_0 = 1$ and all other $\bar{\kappa}_n$ vanish. Analytically, for $\kappa \gg 1$ it is $\kappa_{\pm 1} \simeq \mp \kappa/2$ and $\bar{\kappa}_{\pm 1} \simeq \kappa/2$

After the Cowling theorem we must be interested in growth or decay of a nonaxisymmetric magnetic field. Written with the definitions (19) the resulting equation system for growth or decay of the mode with $m = 1$ (defined by $M = 0$) is

$$\frac{dA_m}{dR} - \left(k^2 + \frac{m^2}{R^2}\right)A_m - \frac{2im}{R^2}B_m -$$

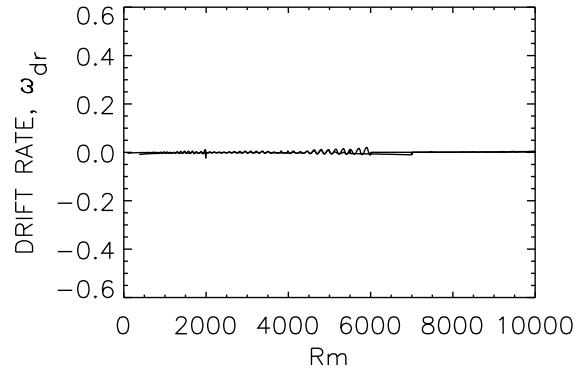
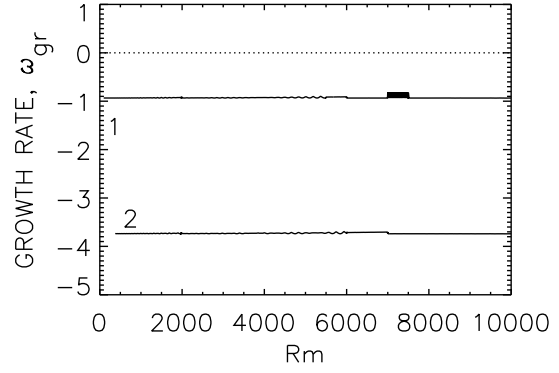


Fig. 3 Growth rate (top) and drift rate (bottom) – both in units of the diffusion rate – for two values of the free axial wave number ($k = 1$ and $k = 2$, marked) for azimuth-dependent electric conductivity. $r_{in} = 0.5$, $\mu = 0.35$ (Kepler rotation). $\kappa = 0.5$, $m = 1$, $M = 1$. Perfect-conducting boundary conditions.

$$\begin{aligned} & - iRm \sum_{n=1-M}^{1+M} \bar{\kappa}_{n-m} (\omega + n\Omega(R) + kU(R)) A_n + \\ & + \sum_{n=1-M}^{1+M} \kappa_{n-m} \left(\frac{nA_n}{R^2} + \frac{iB_n}{R} \right) = 0 \end{aligned} \quad (25)$$

and

$$\begin{aligned} \frac{dB_m}{dR} & - \left(k^2 + \frac{m^2}{R^2}\right)B_m + \frac{2im}{R^2}A_m - \\ & - iRm \sum_{n=1-M}^{1+M} \bar{\kappa}_{n-m} (\omega + n\Omega(R) + kU(R)) B_n - \\ & - 2Rm \frac{b\Omega}{R^2} \sum_{n=1-M}^{1+M} \bar{\kappa}_{n-m} A_n = 0 \end{aligned} \quad (26)$$

formulated for all m with $1 - M \leq m \leq 1 + M$. The number M limits the equation system which is solved if the eigenvalues do no longer depend on the choice of M . It is also possible to consider another nonaxisymmetric mode but here we focus to $m = 1$. The numerical results in Fig. 3 for $\kappa = 0.5$ and with the approximation $M = 1$ for growth rates and drift rates (both normalized with the diffusion frequency) of the eigensolutions are plotted for our

standard container ($r_{\text{in}} = 0.5$) and for Kepler rotation. The resistivity varies in accordance with (23) without any radial variation. The plot shows the eigenfrequencies for the two wave numbers $k = 1$ and $k = 2$. The results are surprising. The modes are always decaying. However, in contrast to the eigenvalues for isolated nonaxisymmetric modes and axisymmetric resistivity with the characteristic Rm behavior shown in Fig. 2 the resulting growth rates in units of the diffusion rate do *not* depend on the magnetic Reynolds number (upper panel) and the decaying patterns do *not* drift in azimuthal direction (lower panel). The nonaxisymmetric η -profile stops the azimuthal drift of the nonaxisymmetric modes and the influence of the differential rotation on the normalized decay rate disappears. Due to the nonaxisymmetric η -profile the $m = 1$ mode is always coupled to the $m = 0$ mode which does not feel the influence of the differential rotation (see Fig. 2, upper panel) and decays only slowly. By the coupling of all the azimuthal modes also the $m = 1$ mode decays as slow as the $m = 0$ mode (see Fig. 3, upper panel)¹.

The upper panel of Fig. 4 shows the growth rates which result from the approximations with $M = 1$ and $M = 2$ for a medium gap with $r_{\text{in}} = 0.5$ and a narrow gap with $r_{\text{in}} = 0.9$. The number of equations strongly grows for growing M . For $M = 1$ the solver works for twelve equations while for $M = 2$ twenty equations are concerned. Nevertheless, the results are very similar, i.e. the growth rates are always negative with almost the same numerical value of order unity. Hence, the modes decay with the diffusion time scale independent of the geometry of the tube and independent of the magnetic Reynolds number Rm . We note that the diffusion time scale is formed with the outer cylinder radius R_0 , the choice of r_{in} does not play a role for the decay rate of the (nonaxisymmetric) mode. Even the rotation law does not play a role as $\mu = 0.35$ only for $r_{\text{in}} = 0.5$ represents a quasi-Kepler rotation but it is a super-Kepler rotation for the more narrow containers with $r_{\text{in}} \geq 0.9$.

In both approximations the decay rates behave very similar. The only difference is a slightly higher decay rate if $M = 2$ which is *unity for all models* if Rm is small. While for the wider gap the curves are strictly horizontal, there may be a little slope for the narrow gaps (see below). The lower panel of Fig. 4 again demonstrates that the considered nonaxisymmetric field with $m = 1$ does not drift in azimuthal direction during its decay. Always the system behaves very similar to the behavior of the mode $m = 0$.

The curves in Fig. 4 do not completely exclude the possibility that for narrow gaps the negative growth rates may change their sign for much higher Rm and a dynamo could start to operate there. For the narrow gap with $r_{\text{in}} = 0.9$ we thus evaluated with Kepler rotation the eigenfrequencies also for very large magnetic Reynolds numbers and for the

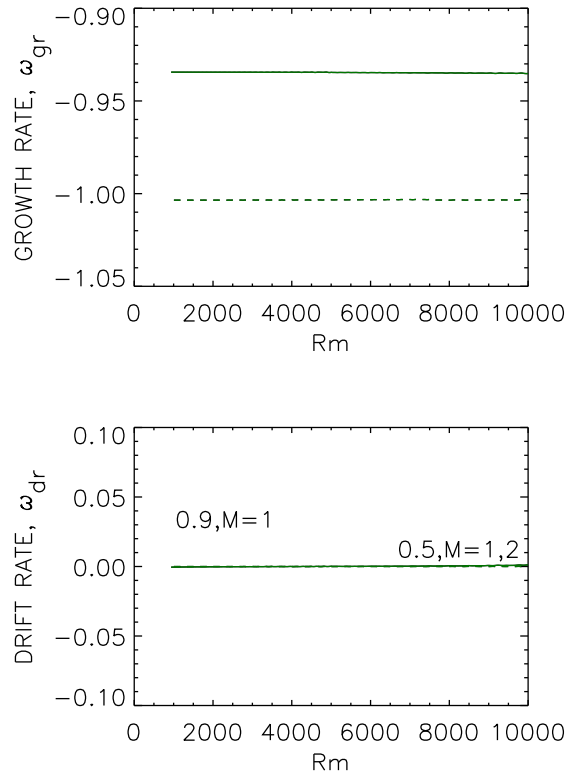


Fig. 4 Growth rates (top) and drift rates (bottom) both normalized with the diffusion frequency for a nonaxisymmetric magnetic field with $m = 1$. Azimuth-dependent electric conductivity with $\kappa = 0.5$ and $M = 1$ (solid) and $M = 2$ (dashed). Two different gap widths: $r_{\text{in}} = 0.5$ (black), $r_{\text{in}} = 0.9$ (green). The curves are completely overlapping. $\mu = 0.35$, $k = 1$. Perfect-conducting boundary conditions.

two resistivity profiles with $\kappa = 0.5$ and $\kappa = 0.95$. $\kappa = 0.5$ describes an azimuthal peak-to-peak variation of the molecular conductivity by a factor of 3 and $\kappa = 0.95$ by a factor of 39. The latter model (thin gap, massive conductivity variations, large magnetic Reynolds numbers) may well approach the assumptions used by Busse & Wicht (1992) in flat geometry. But in cylindrical geometry only negative growth rates are provided for $Rm \leq 10^5$ independent of the actual value of κ (Fig. 5, upper panel). The nonaxisymmetric mode with $m = 1$ just decays with the diffusion time of the purely axisymmetric mode with $m = 0$. The combination of differential rotation and nonuniform molecular conductivity does not lead in our calculations to positive growth rates so that a dynamo does here not exist. Again the azimuthal drift of the magnetic pattern disappears as it does for the decay of the $m = 0$ mode shown in the lower panel of Fig. 1.

We also checked the action of an axial flow $U(R)$ – independent of z – as a function of the radius for the induction equations (25) and (26). It is normalized with the azimuthal flow speed $\Omega_{\text{in}} R_0$, i.e. $U(R) = u_z / \Omega_{\text{in}} R_0$ and its radial

¹ This statement can be probed by solving the system (25) and (26) for $\kappa = 0$ and $M = 0$ which exactly reproduces the red lines in Fig. 2 for the decay of the nonaxisymmetric $m = 1$ mode with uniform resistivity.

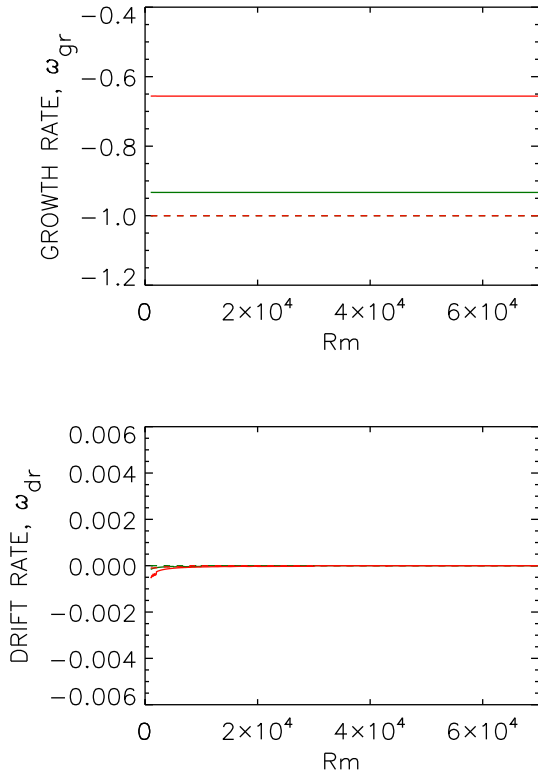


Fig. 5 Similar to Fig. 4 but for very large magnetic Reynolds numbers Rm and with $\kappa = 0.5$ (green) and $\kappa = 0.95$ (red). $M = 1$ (solid), $M = 2$ (dashed). For $M = 2$ the two dashed lines (red and green) are identical. $r_{in} = 0.9$, $\mu = 0.85$ (Kepler rotation), $k = 1$. Perfect-conducting boundary conditions.

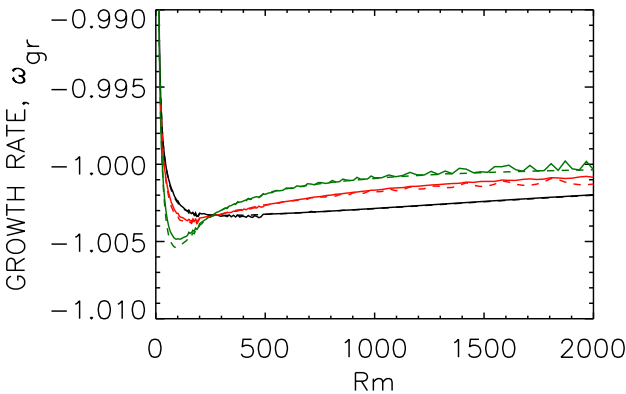


Fig. 6 Growth rates in units of the diffusion rate for various values of the axial flow $-0.5 \leq \hat{U} \leq 0.5$ for $k = 1$ and azimuth-dependent electric conductivity. Solid lines: $\hat{U} > 0$, dashed lines: $\hat{U} < 0$. Green: $|\hat{U}| = 0.5$, red: $|\hat{U}| = 0.25$, black: $|\hat{U}| = 0.1$. $r_{in} = 0.5$, $\mu = 0.35$ (Kepler rotation). $\kappa = 0.5$, $M = 2$. Perfect-conducting boundaries.

profile is simply put to

$$U(R) = \hat{U} \sin \frac{2(R - r_{in})\pi}{1 - r_{in}}. \quad (27)$$

The Fig. 6 demonstrates the irrelevance of such an axial flow (independent of its sign) for the dynamo mechanism what is not surprising. Positive results can only be expected after inclusion of a radial flow but then we would confirm – or not – the results of Dudley & James (1989) for the ability of combined systems of differential rotation and meridional circulations to fulfill the dynamo equation (1) with positive growth rates.

3 Conclusion

We have shown by use of both spherical and cylindrical models that any dependence of the molecular resistivity η on radius or azimuth does not soften the toroidal-velocity anti-dynamo theorem of Elsasser (1946). Our laminar velocity fields do not possess radial components, and hence we do not find any dynamo selfexcitation. Under the exclusive influence of various rotation laws the nonaxisymmetric $m = 1$ mode *decays* for all the considered radial or azimuthal η -profiles and gap widths up to magnetic Reynolds numbers of 10^5 . The decay time equals the diffusion time scale even independent of the amplitude of the azimuthal variation of the the η -profile and also independent of the differential rotation laws.

This finding should be of relevance for the idea that a hot exoplanet develops strong differences of the electric conductivity at their day-side and night-side with the potential to form a magnetic dynamo system (Rogers & McElwaine 2017). After our results this would only be possible if the toroidal-velocity anti-dynamo theorem is overcome by inclusion of a radial flow component but such complex flows after Dudley & James (1989) can generate nonaxisymmetric magnetic fields even without nonuniform molecular conductivity. For the operation of a laminar dynamo the radial flow component cannot successfully be replaced by gradients of the electric conductivity. The idea of Elsasser is confirmed that “it does not seem plausible that this variation introduces phenomena that modify the theory in a fundamental way”.

It remains to probe an axial profile of the molecular resistivity to support dynamo action. This problem does not cover the transformation of the dynamo of Busse & Wicht to cylindrical or spherical geometry. Inspecting the equation system one finds a more complex instability problem. The last term of Eq. (8) for $\eta = \eta(z)$ provides a coupling of the equations via B_z . If ever, the radial magnetic field is exclusively originated by the axial field rather than by the azimuthal field as it is the case for $\eta = \eta(\phi)$. The coupling is thus only weak for dynamos with weak axial fields as it is usually realized for dynamos with differential rotation. As nevertheless such a dynamo cannot be excluded new calculations must provide the consequences of profiles such as $\eta = \eta(z)$, see Marcotte et al. (2021).

Acknowledgement Axel Brandenburg (Stockholm), Rainer Hollerbach (Leeds) and Johannes Wicht (Göttingen) are cordially acknowledged for stimulating discussions.

References

- Brandenburg A., Moss D., Tuominen I., 1992, in Harvey K. L., ed., *The Solar Cycle Vol. 27 of Astronomical Society of the Pacific Conference Series, Turbulent Pumping in the Solar Dynamo*. p. 536
- Busse F. H., Wicht J., 1992, *Geophysical and Astrophysical Fluid Dynamics*, 64, 135
- Dudley M. L., James R. W., 1989, *Proceedings of the Royal Society of London Series A*, 425, 407
- Elsasser W. M., 1946, *Physical Review*, 69, 106
- Gailitis A., 1970, *Magnitnaia Hidrodinamika*, p. 19
- Giesecke A., Nore C., Stefani F., Gerbeth G., Leorat J., Ludens F., Guermond J. L., 2010, *Geophysical and Astrophysical Fluid Dynamics*, 104, 505
- Ivers D. J., James R. W., 1988a, *Geophysical and Astrophysical Fluid Dynamics*, 44, 271
- Ivers D. J., James R. W., 1988b, *Geophysical and Astrophysical Fluid Dynamics*, 40, 147
- Kaiser R., Busse F., 2017, *Geophysical and Astrophysical Fluid Dynamics*, 111, 355
- Krause F., Rädler K. H., 1980, *Mean-field magnetohydrodynamics and dynamo theory*. Pergamon Press Press
- Latter H., Ivers D., 2010, *Physics of Fluids*, 22, 066601
- Marcotte F., Gallet B., Pétrélis F., Gissinger C., 2021, *Physical Review E*, 104, 015110
- Moss D., 2006, *Geophysical and Astrophysical Fluid Dynamics*, 100, 49
- Rogers T. M., McElwaine J. N., 2017, *The Astrophysical Journal Letters*, 841, L26
- Rüdiger G., Gellert M., Hollerbach R., Schultz M., Stefani F., 2018, *Physics reports*, 741, 1
- Shalybkov D. A., Rüdiger G., Schultz M., 2002, *Astronomy & Astrophysics*, 395, 339
- Tan X., Komacek T. D., 2019, *The Astrophysical Journal*, 886, 26